

# Self-ordered Time Crystals: Periodic Temporal Order Under Quasiperiodic Driving

Sayan Choudhury<sup>1,\*</sup> and W. Vincent Liu<sup>1,2,†</sup>

<sup>1</sup>*Department of Physics and Astronomy, University of Pittsburgh, Pittsburgh, PA 15260, USA*

<sup>2</sup>*Department of Physics and Shenzhen Institute for Quantum Science and Engineering, Southern University of Science and Technology, Shenzhen 518055, China*

(Dated: January 8, 2022)

A discrete time crystal is a remarkable non-equilibrium phase of matter characterized by persistent sub-harmonic response to a periodic drive. Motivated by the question of whether such time-crystalline order can persist when the drive becomes aperiodic, we investigate the dynamics of a Lipkin-Meshkov-Glick model under quasiperiodic kicking. Intriguingly, this infinite-range-interacting spin chain can exhibit long-lived periodic oscillations when the kicking amplitudes are drawn from the Thue-Morse sequence (TMS). We dub this phase a “self-ordered time crystal” (SOTC), and demonstrate that our model hosts at least two qualitatively distinct prethermal SOTC phases. These SOTCs are robust to various perturbations, and they originate from the interplay of long-range interactions and the recursive structure of the TMS. Our results suggest that quasiperiodic driving protocols can provide a promising route for realizing novel non-equilibrium phases of matter in long-range interacting systems.

**Introduction:** In recent years, periodic driving has emerged as a powerful tool for the coherent control of quantum many-body systems [1–7]. Periodically driven (Floquet) systems provide a versatile platform for designing quantum many-body states which may not have any equilibrium analog. A particularly intriguing example of such a non-equilibrium phase of matter is a discrete time crystal (DTC) [8–11]. A DTC spontaneously breaks discrete time-translation symmetry (TTS), and consequently exhibits a stable sub-harmonic response of physical observables. Following the first pioneering theoretical proposals [12–16], DTCs have now been realized in several experimental platforms [17–25].

While Floquet engineering protocols are remarkably powerful, they have an inherent drawback - periodic driving typically heats up quantum systems to a featureless infinite temperature state [26, 27]. To circumvent this problem, the first realization of a DTC relied crucially on the presence of many-body localization (MBL) [17]. Many-body localized systems are characterized by an extensive number of emergent local integrals of motion and they do not absorb heat from the drive, thereby providing a robust route to avoid heat death [14]. Furthermore, several recent studies have found that MBL can even stabilize quasiperiodically driven systems [28–34], leading to the emergence of novel prethermal phases of matter like a “time quasicrystal” [29, 30].

Unfortunately, the requirement of MBL places very restrictive constraints on the strength and range of interactions [35–38]. This issue has necessitated the search for other pathways to stabilize a DTC. In an encouraging development, several researchers have recently demonstrated the possibility of realizing a DTC in the absence of disorder [39–49]. These disorder-free DTCs inherit their stability from intriguing mechanisms like emergent integrability [39], quantum many-body echo [46, 47], long-range interactions [49, 50], prethermaliza-

tion without temperature [19, 51], and many-body scarring [52, 53]. These time crystals are robust to various perturbations that preserve the perfect periodicity of the external drive. An intriguing question naturally arises in this context: can such time crystals spontaneously emerge when the drive becomes aperiodic in nature?

In this Letter, we answer this question affirmatively by demonstrating that time crystals can emerge in a quasiperiodically kicked Lipkin-Meshkov-Glick (LMG) model [54]. We note that this infinite-range interacting spin chain can exhibit integrable dynamics and robust DTC order under an appropriate Floquet protocol [40, 49]. However, quasiperiodically kicked systems are generally expected to heat up much faster than their Floquet counterparts, due to the presence of multiple incommensurate frequencies in the drive. Rather surprisingly, we find that this chain exhibits robust periodic oscillations akin to a DTC for a wide parameter regime; this phase is designated as a “self-ordered-time-crystal” (SOTC). Furthermore, due to the infinite-range nature of the Ising interaction, we can establish the stability of this phase in the thermodynamic limit, thus allowing us to avoid any erroneous conclusions that can arise from finite size numerics. Finally, we note that this model can be realized in a variety of quantum emulator platforms, thereby making our proposal amenable to near-term experimental realizations.

**Model:** We study a kicked LMG chain describing the dynamics of  $L$  spin-1/2 particles mutually interacting through an infinite range Ising interaction subjected to time-dependent transverse magnetic field:

$$H = \frac{J}{2L} \sum_{i=1}^L \sum_{j=1}^L \sigma_i^z \sigma_j^z + \left( \frac{\pi}{m} (1 - \epsilon \tau_n) \delta(t - nT) \right) \sum_i \sigma_i^x, \quad (1)$$

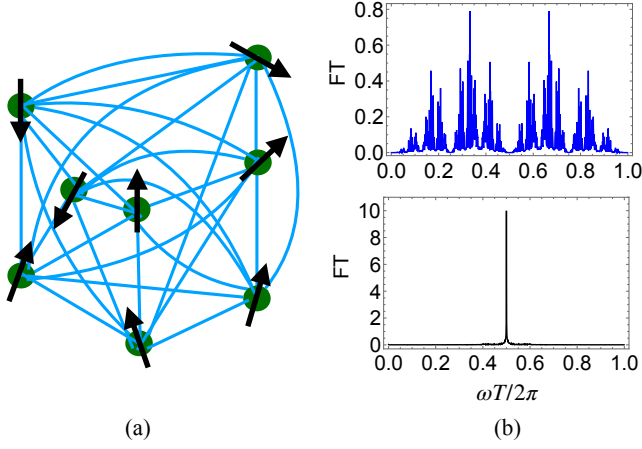


FIG. 1. **Model and dynamical behavior:** (a) Schematic of the quasiperiodically driven infinite range interacting Ising model in Eq. 1. (b) The top (bottom) panel represents the Fourier spectrum of the drive (the response function,  $S^z(t)$  defined in Eq. 3), when  $\epsilon = 0.07$  and  $J = 0.35$  for a 300-site system. The system can exhibit SOTC dynamics with a frequency  $\omega = \pi/T$ , even when the drive is quasiperiodic.

where  $\sigma_i^\gamma$  are the standard Pauli matrices, and  $\tau_n$  is  $n$ -th element of the quasiperiodic Thue-Morse sequence (TMS). A schematic of this model is shown in Fig. 1(a).

The TMS is composed of an infinite number of successive subsequences, where the  $\mu$ -th subsequence, comprises  $2^\mu$  elements as follows [55, 56]:

$$s(\mu) = s(\mu-1)s_{1/2}^R(\mu-1)s_{1/2}^L(\mu-1) \quad (2)$$

where,  $s_{1/2}^R(s_{1/2}^L)$  denote the right (left) half of the sub-sequence and  $s_1 = \{0, 1\}$ . Thus, the first few values of the TMS are  $\{\{0, 1\}, \{0, 1, 1, 0\}, \{0, 1, 1, 0, 1, 0, 0, 1\} \dots$  (see Supplementary Material for a more detailed enumeration of the TMS). This recursive structure makes the TMS quasiperiodic in nature; the Fourier spectrum of this sequence is shown in the top panel of Fig. 1(b). We note that in the absence of any external drive, this model is mean-field solvable in the thermodynamic limit. Intriguingly, this feature protects the periodically kicked LMG chain from heat death, and enables it to exhibit robust DTC order for several values of  $m$  [49]. We focus on the  $m = 2$  and  $m = 4$  case in this work.

**Non-equilibrium Phases:** In order to characterize the dynamical phases of our model, we examine the dynamics of the average  $z$ -magnetization:

$$S^z(t) = \frac{1}{L} \sum_j \langle \psi | S_j^z(t) | \psi \rangle, \quad (3)$$

when the initial state is fully polarized,  $|\psi\rangle = |\uparrow\uparrow\uparrow \dots \uparrow\uparrow\rangle$  and  $S_j^z = \frac{1}{2}\sigma_j^z$ . This order parameter been conventionally used to identify the DTC and time quasicrystal phases. Furthermore, since the total spin operator  $S^2$

(where  $\vec{S} = \frac{1}{2} \sum_j (\hat{x}\sigma_j^x + \hat{y}\sigma_j^y + \hat{z}\sigma_j^z)$ ) commutes with  $H$ , this choice of initial state ensures that the dimension of the effective Hilbert space is  $L + 1$  (instead of  $2^L$ ), thus enabling us to access large system sizes using exact diagonalization (ED). We note that other authors have employed a similar strategy to establish the existence of DTC phases in the Floquet LMG chain [40, 49].

Our calculations reveal that this spin chain can exhibit two qualitatively different kinds of time crystal behavior when  $\epsilon$  is small (see Fig. 2): (a) the SOTC-I phase where the Fourier transform of  $S^z(t)$  has a sharp peak at a frequency  $\frac{\pi}{T}$  (when  $m = 2$ ) in a manner similar to a period doubling DTC, and (b) the SOTC-II phase characterized by sharp Fourier peaks at the frequencies of  $\frac{\pi}{2T}$  and  $\frac{3\pi}{2T}$  (when  $m = 4$ ), akin to a higher-order time crystal.

In order to characterize this novel phase further, we examine the system size dependence of the lifetime of the sub-harmonic oscillations. As shown in Fig. 2(a1), this lifetime (defined as the earliest time  $n^*T$ , when  $|S^z(n^*T)| \leq 0.05$ ) appears to be independent of the length of the chain, thereby indicating that this phase is prethermal. More generally, unlike DTCs which can maintain quantum coherence up to infinitely long times in the thermodynamic limit, it is (almost) impossible to evade eventual heat death when the drive is quasiperiodic [31, 34, 57–59].

The emergence of the SOTC phase in the preheating regime can be understood by employing a high frequency approximation. To see this, we first note that the time evolution operator is composed of a quasiperiodic sequence of two types of effective “dipoles”,  $U_+ = U_0 U_1$  and  $U_- = U_1 U_0$  [59], where:

$$U_0 = \bar{U} \exp\left(-i\frac{\pi}{2}\frac{\epsilon}{2} \sum_j \sigma_j^x\right), U_1 = \bar{U} \exp\left(i\frac{\pi}{2}\frac{\epsilon}{2} \sum_j \sigma_j^x\right),$$

and

$$\bar{U} = \exp\left(-i\frac{JT}{L} \sum_{j,l} \sigma_j^z \sigma_l^z\right) \exp\left(-i\frac{\pi}{2}\left(1 - \frac{\epsilon}{2}\right) \sum_j \sigma_j^x\right). \quad (4)$$

In the high-frequency ( $JT \ll 1$ ) and small  $\epsilon$  ( $\pi\epsilon \ll 1$ ) limit,  $U_+ \approx U_- \approx \bar{U}^2$ , and the evolution of the spin chain is approximately described by the Floquet propagator  $\bar{U}$ . This simplification leads to a remarkable conclusion: this system can be a SOTC and exhibit long-lived periodic oscillations in the same parameter regimes, where the Floquet LMG chain exhibited DTC dynamics.

To obtain the phase diagram, we compute an appropriate long-time average of the SOTC order parameters:

$$Z_2 = \frac{1}{N} \sum_{n=0}^N (-1)^n S^z(nT); Z_4 = \frac{2}{N} \sum_{n=0}^{N/2} (-1)^n S^z(2nT), \quad (5)$$

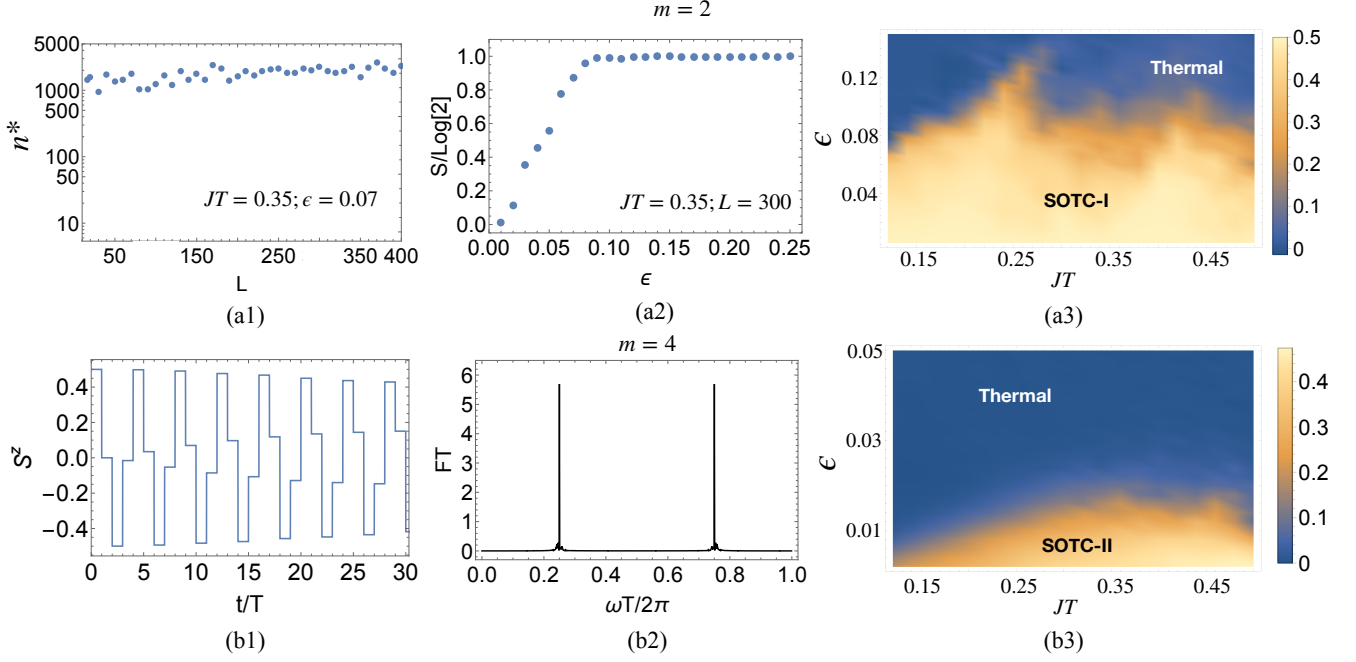


FIG. 2. **Dynamical phases of the driven spin chain** (a1) The SOTC lifetime,  $n^*$  as a function of the system size. The lifetime seems to be independent of the system size, thereby indicating that the phase is pre-thermal. (a2) The single site entanglement entropy of the system,  $S$  as a function of  $\epsilon$  - the transition from the SOTC-I phase to the thermal phase is accompanied by an increase in  $S$  from 0 to  $\log(2)$ . (a3) The dynamical phase diagram of this spin chain, obtained by averaging the order parameter  $Z_2$  (defined in Eq. 5) from  $t = 0$  to  $t = 1000T$ . (b1) The time-evolution of the  $z$ -magnetization,  $S^z$  (defined in Eq. 3) in the SOTC-II phase. (b2) The Fourier transform of  $S^z(t)$  shows a sharp Fourier peak at  $\omega = \frac{\pi}{4T}$  and  $\omega = \frac{3\pi}{4T}$  in the small  $\epsilon$  regime, establishing the presence of the SOTC-II phase. (b3) The phase diagram obtained by averaging  $Z_4$  (defined in Eq. 5) from  $t = 0$  to  $t = 500T$ .

where  $N$  is the total number of kicks and  $Z_2(Z_4)$  corresponds to the SOTC-I (SOTC-II) phase. As shown in Fig. 2, the spin chain is a SOTC for a wide parameter regime; this phase is characterized by a large value of  $Z$  ( $\sim 0.5$ ) for  $N \gg 1$ . We note that at sufficiently long times however, the mapping to the Floquet LMG chain breaks down, and the system thermalizes.

The aforementioned analysis can not capture the dynamics of the system when  $\epsilon$  is large ( $\pi\epsilon \sim 1$ ). By carefully studying this regime, we have found that in this case, the Fourier spectrum comprises multiple broad peaks,  $Z_m = 0$ , and the single site entanglement entropy,  $S = \rho_i \log(\rho_i)$  is maximal  $\sim \log(2)$  ( $\rho_i$  is the reduced density matrix at site  $i$ ), thereby establishing that the system is in the thermal phase (see Fig. 2(a2)). While the results shown here are for finite, albeit large size chains, we have also confirmed that the observed SOTC behavior persists in the thermodynamic limit. Interestingly, signatures of the SOTC-I phase can also be seen for small system sizes, while the SOTC-II only emerges for large system sizes ( $L \sim 100$ ) (see Supplementary Material).

Since the SOTC is a prethermal phase, it is natural that the lifetime of the oscillations would depend strongly

on the energy of the initial state, defined as follows:

$$E = \langle \psi(t=0) | \frac{J}{L} \sum_{i,j} \sigma_i^z \sigma_j^z | \psi(t=0) \rangle, \quad (6)$$

To characterize this dependence, we have examined the time evolution of this model starting from various initial states. As shown in Fig. 3, the SOTC lifetime shows a clear dependence on the initial state: it is maximum for the globally polarized state and it decreases monotonically with decreasing energy (and initial  $z$ -magnetization,  $S^z(t=0)$ ). Recently, Kyprianidis *et al.* [60] have discovered that prethermal DTCs in long-range interacting Ising spin chains exhibit qualitatively similar behavior.

Finally, we investigate the robustness of this phase by studying the response of this spin chain when the time-independent part of the Hamiltonian is no longer mean-field solvable. In particular, we examine the response of this spin chain to two kind of perturbations: (a) when the long-range Ising interaction decays as a power law, or (b) when an additional nearest-neighbor Ising interaction is present. This analysis can be performed succinctly by

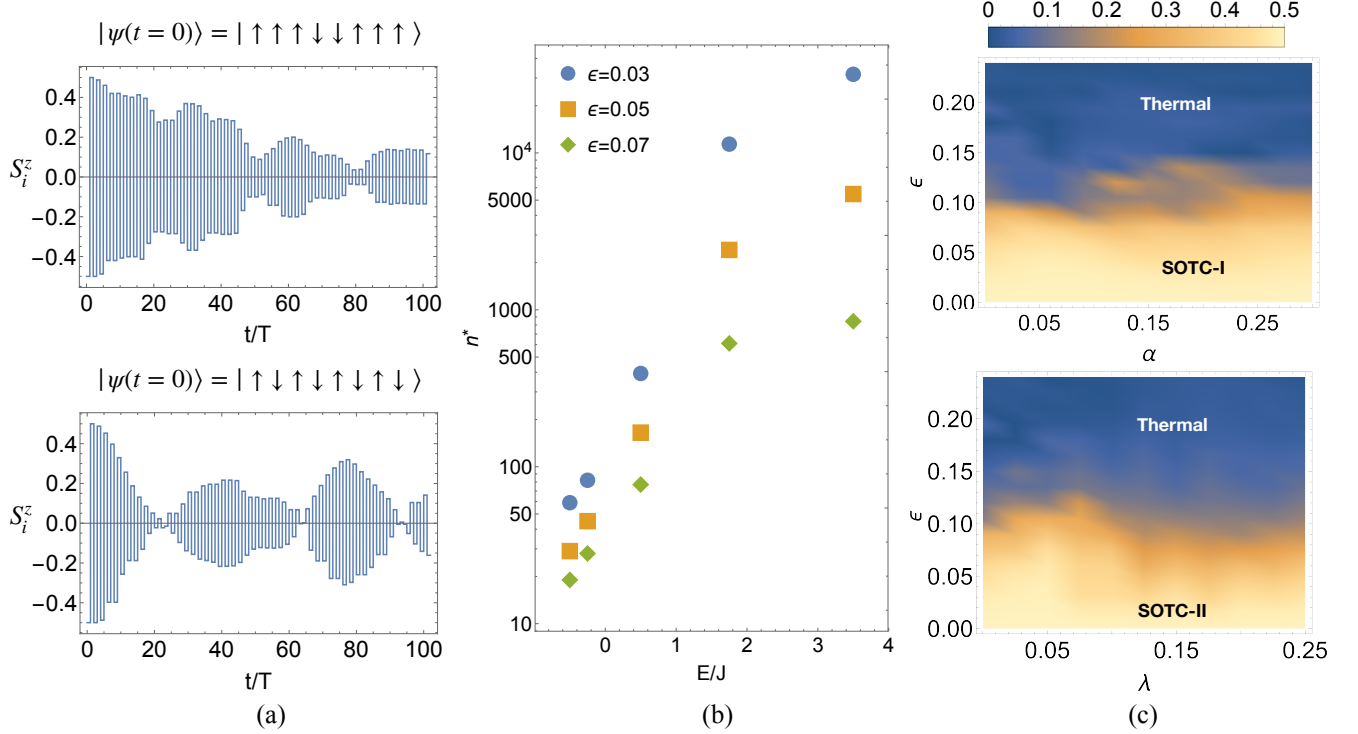


FIG. 3. **Other initial states and robustness to perturbations:** (a) The local  $z$ -magnetization of the  $i$ -th spin,  $S_i^z(t)$  for other initial states, when  $L = 8$ . We show the results for  $i = 4$  here, though similar results are found for any value of  $i$ . The lifetime of the periodic oscillations shows a strong dependence on the energy of the initial state. This is a clear signature of a prethermal state. (b) Dependence of the SOTC lifetime on the energy  $E$  (see Eq. 6) of the initial state. The lifetime increases with increasing  $E$  and decreasing  $\epsilon$ . (c) The phase diagram of the model when the initial state is globally polarized obtained by averaging  $Z_2$  from  $t = 0$  to  $1000T$  evolving under the Hamiltonian  $H_{\alpha,\lambda}$  defined in Eq. 7. It is clear that the system can exhibit SOTC-I behavior for a wide range of perturbations

studying the evolution of the following Hamiltonian:

$$H_{\alpha,\lambda} = \sum_{i,j} \frac{J}{L|j-i|^\alpha} \sigma_i^z \sigma_j^z + \lambda \sigma_i^z \sigma_{i+1}^z + \sum_i \left( \frac{\pi}{m} \delta(t - nT) - \epsilon(t) \right) \sum_i \sigma_i^x, \quad (7)$$

As shown in Fig. 3(c), we find that the SOTC remains stable in the presence of these perturbations.

**Experimental Realizations:** The time-independent part of the Hamiltonian in Eq. 1 is an infinite-range interacting Ising model, and it arises naturally as the effective model describing the dynamics of an ensemble of spins coupled to a single mode cavity in the “bad cavity” regime [61]. A similar strategy can be employed to emulate this model using superconducting quantum processors. Alternatively, this model can be engineered in a trapped ion crystal using both analog and digital quantum simulation techniques [62–64]. Another promising route to realize this model is provided by ultracold bosonic atoms loaded in a double well potential [65]. In this case, the two wells can be mapped to spin-up and down respectively, while the tunneling between the

wells plays the role of the transverse magnetic field. In all of these implementations, the toolbox developed for periodically driving the transverse magnetic field can potentially be employed to make the drive quasiperiodic in nature (see Supplementary Material for a more detailed description of potential experimental realizations of our proposal). Finally, we note that the time evolution of the total magnetization is routinely studied in the aforementioned quantum emulator platforms.

**Summary and Outlook:** Time crystals epitomize the profound principle of time-translation symmetry breaking in quantum many-body systems. In this work, we have introduced a new class of prethermal time crystals - the “self-ordered time crystal” - that emerges in a quasi-periodically kicked spin chain. This novel non-equilibrium state is stabilized by the interplay of the Thue-Morse driving and long-range interactions. We emphasize that SOTCs are qualitatively distinct from MBL-DTCs, whose robustness is guaranteed only when the drive is perfectly periodic [14].

We have systematically studied the dependence of the SOTC dynamics on the initial state and found that

the lifetime increases with increasing energy and spin-polarization. Furthermore, we have demonstrated that this SOTC phase can persist in the thermodynamic limit, and it remains stable under various perturbations. Finally, we have discussed possible experimental realizations of this model. Our work clearly demonstrates that quasiperiodically driven many-body systems can host a rich array of non-equilibrium phases.

There are several possible extensions of this work. One promising direction is to examine routes to realize a SOTC in the presence of dissipation [24]. More generally, it would be interesting to explore the dynamics of long-range interacting spin chains subjected to different forms of quasiperiodic drive [66, 67], as well as dissipation [68]. Alternatively, it would be intriguing to investigate schemes to leverage quasiperiodic driving for quantum-enhanced metrology [69].

The authors want to thank Biao Huang for helpful discussions. This work is supported by the AFOSR Grant No. FA9550-16-1-0006, the MURI-ARO Grant No. W911NF17-1-0323 through UC Santa Barbara, and the Shanghai Municipal Science and Technology Major Project through the Shanghai Research Center for Quantum Sciences (Grant No. 2019SHZDZX01).

---

\* sayan.choudhury@pitt.edu

† wvliu@pitt.edu

- [1] A. Eckardt, C. Weiss, and M. Holthaus, *Phys. Rev. Lett.* **95**, 260404 (2005).
- [2] M. Holthaus, *J. Phys. B* **49**, 013001 (2015).
- [3] M. Bukov, L. D'Alessio, and A. Polkovnikov, *Adv. Phys.* **64**, 139 (2015).
- [4] A. Eckardt, *Rev. Mod. Phys.* **89**, 011004 (2017).
- [5] T. Oka and S. Kitamura, *Annu. Rev. Condens. Matter Phys.* **10**, 387 (2019).
- [6] R. Moessner and S. L. Sondhi, *Nat. Phys.* **13**, 424 (2017).
- [7] M. S. Rudner and N. H. Lindner, *Nat. Rev. Phys.* **2**, 229 (2020).
- [8] K. Sacha and J. Zakrzewski, *Rep. Prog. Phys.* **81**, 016401 (2017).
- [9] K. Sacha, *Time Crystals*, Springer Series on Atomic, Optical, and Plasma Physics, Vol. 114 (Springer, Cham, Switzerland, 2020).
- [10] V. Khemani, R. Moessner, and S. L. Sondhi, *arXiv:1910.10745* (2019).
- [11] D. V. Else, C. Monroe, C. Nayak, and N. Y. Yao, *Annu. Rev. Condens. Matter Phys.* **11**, 467 (2020).
- [12] K. Sacha, *Phys. Rev. A* **91**, 033617 (2015).
- [13] V. Khemani, A. Lazarides, R. Moessner, and S. L. Sondhi, *Phys. Rev. Lett.* **116**, 250401 (2016).
- [14] C. W. von Keyserlingk, V. Khemani, and S. L. Sondhi, *Phys. Rev. B* **94**, 085112 (2016).
- [15] D. V. Else, B. Bauer, and C. Nayak, *Phys. Rev. Lett.* **117**, 090402 (2016).
- [16] N. Y. Yao, A. C. Potter, I.-D. Potirniche, and A. Vishwanath, *Phys. Rev. Lett.* **118**, 030401 (2017).
- [17] J. Zhang, P. Hess, A. Kyprianidis, P. Becker, A. Lee, J. Smith, G. Pagano, I.-D. Potirniche, A. C. Potter, A. Vishwanath, N. Y. Yao, and C. Monroe, *Nature* **543**, 217 (2017).
- [18] S. Choi, J. Choi, R. Landig, G. Kucsko, H. Zhou, J. Isoya, F. Jelezko, S. Onoda, H. Sumiya, V. Khemani, C. von Keyserlingk, N. Y. Yao, E. Demler, and M. D. Lukin, *Nature* **543**, 221 (2017).
- [19] J. Rovny, R. L. Blum, and S. E. Barrett, *Phys. Rev. Lett.* **120**, 180603 (2018).
- [20] S. Pal, N. Nishad, T. Mahesh, and G. Sreejith, *Phys. Rev. Lett.* **120**, 180602 (2018).
- [21] J. O'Sullivan, O. Lunt, C. W. Zollitsch, M. L. W. Thewalt, J. J. L. Morton, and A. Pal, *New J. Phys.* **22**, 085001 (2020).
- [22] H. Keßler, J. G. Cosme, C. Georges, L. Mathey, and A. Hemmerich, *New J. Phys.* **22**, 085002 (2020).
- [23] J. Randall, C. E. Bradley, F. V. van der Gronden, A. Galicia, M. H. Abobeih, M. Markham, D. J. Twitchen, F. Machado, N. Y. Yao, and T. H. Taminiau, *arXiv preprint arXiv:2107.00736* (2021).
- [24] H. Keßler, P. Kongkhambut, C. Georges, L. Mathey, J. G. Cosme, and A. Hemmerich, *Phys. Rev. Lett.* **127**, 043602 (2021).
- [25] X. Mi, M. Ippoliti, C. Quintana, A. Greene, Z. Chen, J. Gross, F. Arute, K. Arya, J. Atalaya, R. Babbush, *et al.*, *arXiv preprint arXiv:2107.13571* (2021).
- [26] L. D'Alessio and M. Rigol, *Phys. Rev. X* **4**, 041048 (2014).
- [27] A. Lazarides, A. Das, and R. Moessner, *Phys. Rev. E* **90**, 012110 (2014).
- [28] H. Zhao, F. Mintert, and J. Knolle, *Phys. Rev. B* **100**, 134302 (2019).
- [29] P. T. Dumitrescu, R. Vasseur, and A. C. Potter, *Phys. Rev. Lett.* **120**, 070602 (2018).
- [30] D. V. Else, W. W. Ho, and P. T. Dumitrescu, *Phys. Rev. X* **10**, 021032 (2020).
- [31] B. Lapierre, K. Choo, A. Tiwari, C. Tauber, T. Neupert, and R. Chitra, *Phys. Rev. Research* **2**, 033461 (2020).
- [32] A. J. Friedman, B. Ware, R. Vasseur, and A. C. Potter, *arXiv:2009.03314* (2020).
- [33] B. Mukherjee, A. Sen, D. Sen, and K. Sengupta, *Phys. Rev. B* **102**, 014301 (2020).
- [34] X. Wen, R. Fan, A. Vishwanath, and Y. Gu, *Phys. Rev. Research* **3**, 023044 (2021).
- [35] S. Gopalakrishnan and S. A. Parameswaran, *Physics Reports* **862**, 1 (2020).
- [36] D. A. Abanin, E. Altman, I. Bloch, and M. Serbyn, *Reviews of Modern Physics* **91**, 021001 (2019).
- [37] A. Morningstar, L. Colmenarez, V. Khemani, D. J. Luitz, and D. A. Huse, *arXiv preprint arXiv:2107.05642* (2021).
- [38] M. Kiefer-Emmanouilidis, R. Unanyan, M. Fleischhauer, and J. Sirker, *Physical Review B* **103**, 024203 (2021).
- [39] B. Huang, Y.-H. Wu, and W. V. Liu, *Phys. Rev. Lett.* **120**, 110603 (2018).
- [40] A. Russomanno, F. Iemini, M. Dalmonte, and R. Fazio, *Phys. Rev. B* **95**, 214307 (2017).
- [41] K. Mizuta, K. Takasan, M. Nakagawa, and N. Kawakami, *Phys. Rev. Lett.* **121**, 093001 (2018).
- [42] W. C. Yu, J. Tangpanitanon, A. W. Glaetzle, D. Jaksch, and D. G. Angelakis, *Phys. Rev. A* **99**, 033618 (2019).
- [43] F. M. Surace, A. Russomanno, M. Dalmonte, A. Silva, R. Fazio, and F. Iemini, *Phys. Rev. B* **99**, 104303 (2019).
- [44] A. Pizzi, J. Knolle, and A. Nunnenkamp, *Phys. Rev. Lett.* **123**, 150601 (2019).

- [45] A. Kshetrimayum, J. Eisert, and D. Kennes, *Physical Review B* **102**, 195116 (2020).
- [46] C. Lyu, S. Choudhury, C. Lv, Y. Yan, and Q. Zhou, *Phys. Rev. Research* **2**, 033070 (2020).
- [47] S. Choudhury, *Atoms* **9**, 25 (2021).
- [48] A. Pizzi, D. Malz, G. De Tomasi, J. Knolle, and A. Nunnenkamp, *Phys. Rev. B* **102**, 214207 (2020).
- [49] A. Pizzi, J. Knolle, and A. Nunnenkamp, *Nat. Commun.* **12**, 1 (2021).
- [50] X. Yang and Z. Cai, *Phys. Rev. Lett.* **126**, 020602 (2021).
- [51] D. J. Luitz, R. Moessner, S. Sondhi, and V. Khemani, *Phys. Rev. X* **10**, 021046 (2020).
- [52] H. Yarloo, A. E. Kopaei, and A. Langari, *Phys. Rev. B* **102**, 224309 (2020).
- [53] N. Maskara, A. A. Michailidis, W. W. Ho, D. Bluvstein, S. Choi, M. D. Lukin, and M. Serbyn, *arXiv:2102.13160* (2021).
- [54] H. J. Lipkin, N. Meshkov, and A. Glick, *Nucl. Phys.* **62**, 188 (1965).
- [55] A. Thue, *Norske Vid Selsk. Skr. I Mat-Nat Kl.(Christiana)* **7**, 1 (1906).
- [56] H. M. Morse, *Transactions of the American Mathematical Society* **22**, 84 (1921).
- [57] S. Nandy, A. Sen, and D. Sen, *Physical Review X* **7**, 031034 (2017).
- [58] S. Nandy, A. Sen, and D. Sen, *Phys. Rev. B* **98**, 245144 (2018).
- [59] H. Zhao, F. Mintert, R. Moessner, and J. Knolle, *Phys. Rev. Lett.* **126**, 040601 (2021).
- [60] A. Kyprianidis, F. Machado, W. Morong, P. Becker, K. S. Collins, D. V. Else, L. Feng, P. W. Hess, C. Nayak, G. Pagano, N. Y. Yao, and C. Monroe, *Science* **372**, 1192 (2021).
- [61] J. A. Muniz, D. Barberena, R. J. Lewis-Swan, D. J. Young, J. R. Cline, A. M. Rey, and J. K. Thompson, *Nature* **580**, 602 (2020).
- [62] R. Islam, C. Senko, W. Campbell, S. Korenblit, J. Smith, A. Lee, E. Edwards, C.-C. J. Wang, J. K. Freericks, and C. Monroe, *Science* **340**, 583 (2013).
- [63] B. P. Lanyon, C. Hempel, D. Nigg, M. Müller, R. Gerritsma, F. Zähringer, P. Schindler, J. T. Barreiro, M. Rambach, G. Kirchmair, M. Hennrich, P. Zoller, R. Blatt, and C. F. Roos, *Science* **334**, 57 (2011).
- [64] R. Blatt and C. F. Roos, *Nat. Phys.* **8**, 277 (2012).
- [65] M. Albiez, R. Gati, J. Fölling, S. Hunsmann, M. Cristiani, and M. K. Oberthaler, *Phys. Rev. Lett.* **95**, 010402 (2005).
- [66] S. Ray, S. Sinha, and D. Sen, *Phys. Rev. E* **100**, 052129 (2019).
- [67] S. Maity, U. Bhattacharya, A. Dutta, and D. Sen, *Phys. Rev. B* **99**, 020306 (2019).
- [68] S. Schütz, S. B. Jäger, and G. Morigi, *Physical Review Letters* **117**, 083001 (2016).
- [69] S. Choi, N. Y. Yao, and M. D. Lukin, *arXiv:1801.00042* (2017).
- [70] C. Monroe, W. C. Campbell, L.-M. Duan, Z.-X. Gong, A. V. Gorshkov, P. W. Hess, R. Islam, K. Kim, N. M. Linke, G. Pagano, P. Richerme, C. Senko, and N. Y. Yao, *Reviews of Modern Physics* **93**, 025001 (2021).



# Supplementary Material for “Self-ordered Time Crystals: Periodic Temporal Order Under Quasiperiodic Driving”

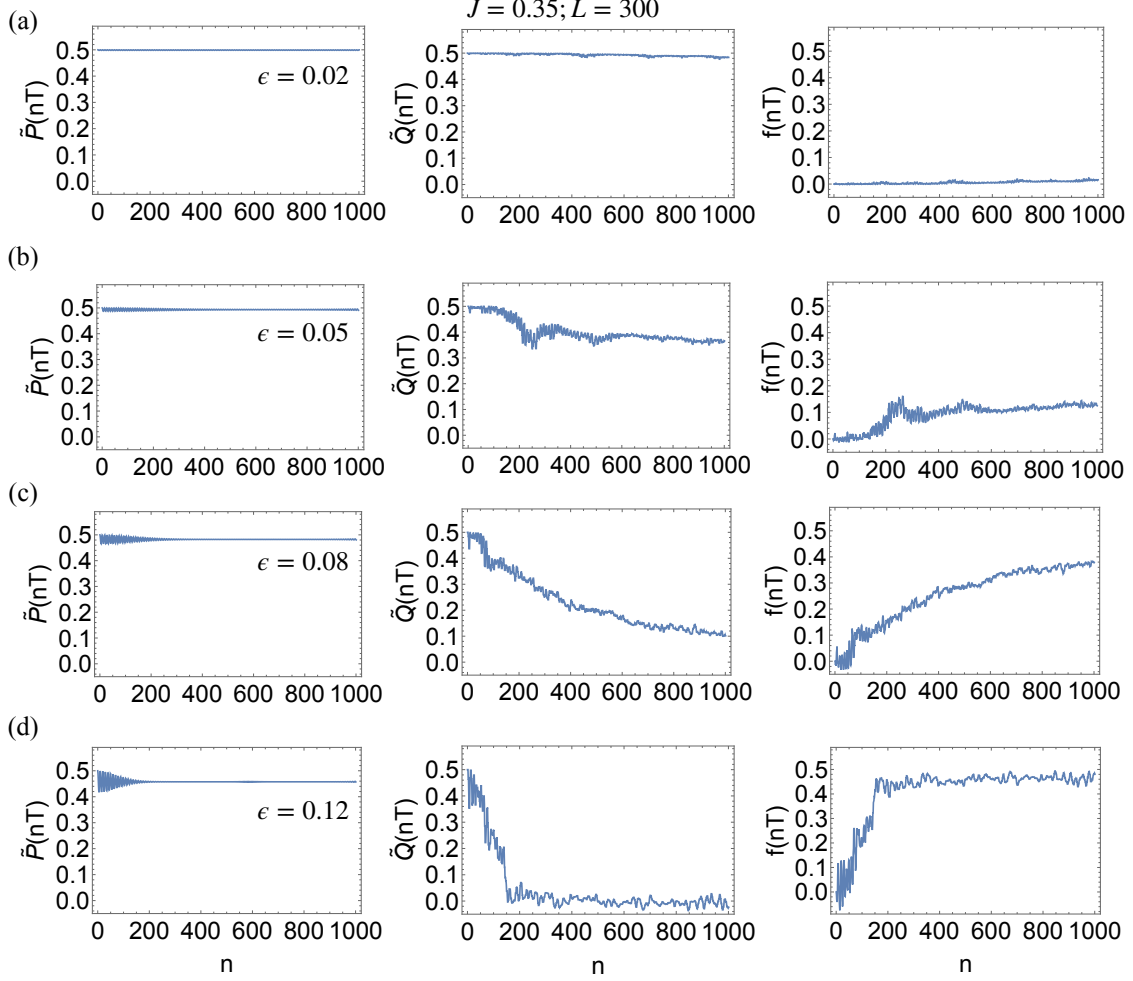


FIG. S1. **Comparison of the dynamics of the periodically and quasiperiodically driven LMG chain:** The order parameters  $\tilde{P}(nT)$ ,  $\tilde{Q}(nT)$  and captures the time evolution of the  $z$ -magnetization in the case of periodic and quasiperiodic drive respectively, and  $f(nT)$  is the difference between  $\tilde{P}(nT)$  and  $\tilde{Q}(nT)$  (see Eq. S1)

## THE THUE-MORSE SEQUENCE

We had described the Thue-Morse sequence (TMS) as a quasiperiodic sequence composed of an infinite number of sub-sequences in Eq. 2 of the main text. Here, we explicitly enumerate the first few subsequences of the TMS:

$$\begin{aligned}\mu = 1 &: 0, 1 \\ \mu = 2 &: 0, 1, 1, 0 \\ \mu = 3 &: 0, 1, 1, 0, 1, 0, 0, 1 \\ \mu = 4 &: 0, 1, 1, 0, 1, 0, 0, 1, 1, 0, 1, 0, 1, 1, 0\end{aligned}$$

The self-similarity of the TMS can be seen by observing that removing every second element of the sequence results in the same sequence. This self-similarity lends the TMS its quasiperiodicity. It is also evident from this structure that the sequence is composed of “effective dipoles”, thus enabling us to perform the effective Floquet analysis performed in the main text. We have compute the following quantities to compare the time-evolution of the  $z$ -magnetization

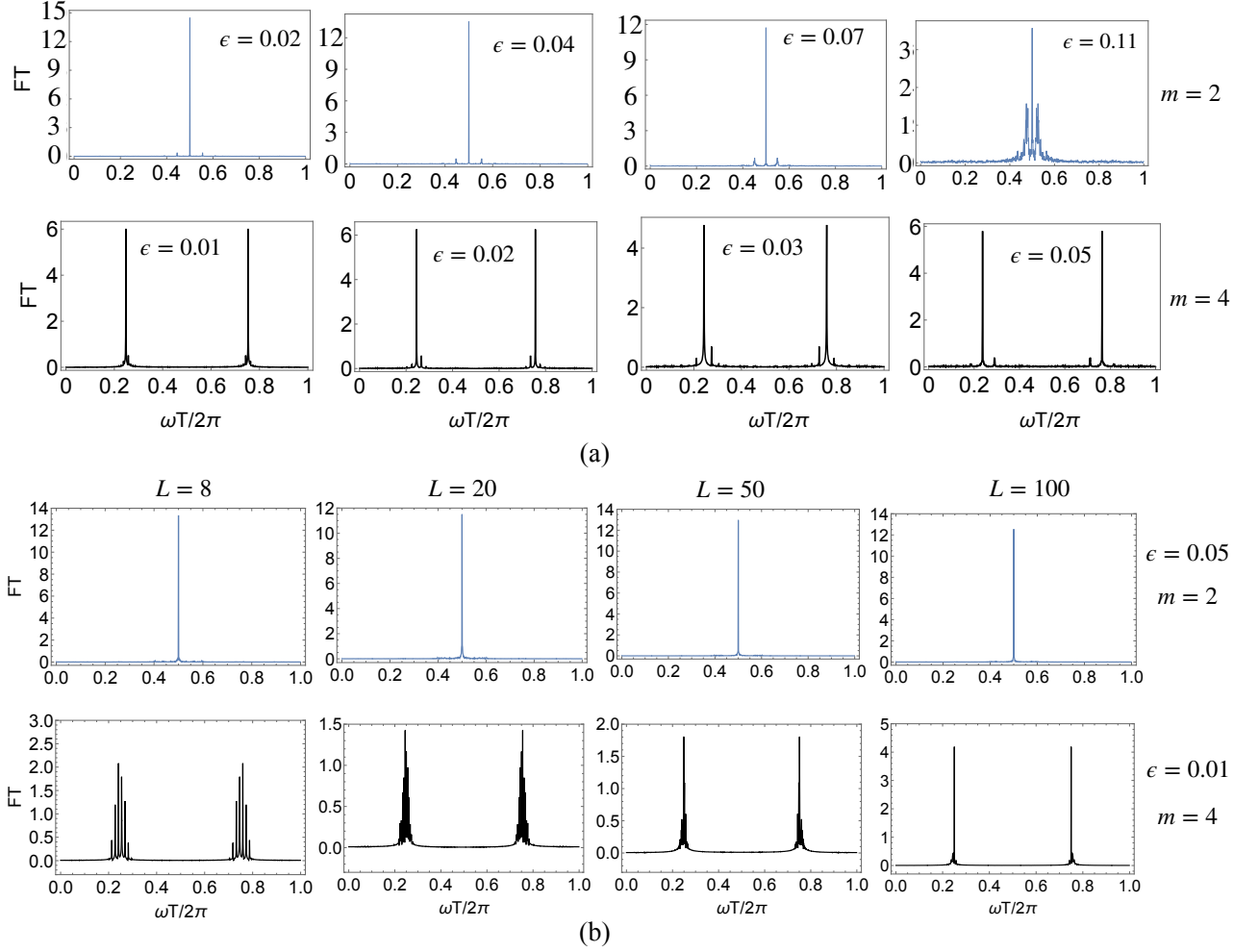


FIG. S2. **Classical results:** (a) The Fourier transform of  $S^z(t)$  in the thermodynamic limit (as captured by Eq. S2). The spin chain is in the SOTC phase in the small- $\epsilon$  regime and it thermalizes in the large- $\epsilon$  regime. (b) The Fourier transform of  $S^z(t)$  as a function of the system size. The SOTC-I appears even for small system sizes, while the SOTC-II only emerges when the system size is large ( $L \sim 100$ )

in this model with that of its effective Floquet counterpart:

$$\tilde{P}(nT) = |\langle \psi | \bar{U}^{\dagger n} S^z(t=0) \bar{U}^n | \psi \rangle|; \tilde{Q}(nT) = |\langle \psi | S^z(nT) | \psi \rangle|; f(nT) = \tilde{P}(nT) - \tilde{Q}(nT). \quad (\text{S1})$$

As shown in Fig. S1, in the SOTC regime,  $\tilde{P}(nT) \sim \tilde{Q}(nT)$  and  $f(nT) \ll 0.5$  up to very long times. In the thermal regime on the other hand  $\tilde{Q}(nT) \sim 0$  and  $\tilde{f}(nT) \sim 0.5$ , even when  $\tilde{P}(nT) \sim 0.5$ .

## CLASSICAL ANALYSIS

The stability of disorder-free DTCs in the limit of infinite system size has given rise to extensive debate in the recent past. In particular, have recently argued that it may even be impossible to realize robust DTCs in short range interacting spin chains in the absence of MBL. Naturally, it is crucial to examine whether the observed SOTC dynamics persists in the thermodynamic limit. Thankfully this issue can be addressed in a straightforward manner in the LMG chain, where the model can be analyzed directly in the thermodynamic limit using semi-classical methods. since the stroboscopic evolution of  $S^z(t)$  in the thermodynamic limit can be captured by the semi-classical equation:

$$S^z((n+1)T) = S^y(nT) \sin(\theta_n) + S^z(nT) \cos(\theta_n), \quad (\text{S2})$$



where  $\theta_n = \frac{2\pi}{m}(1 - \epsilon\tau_n)$ , and the  $\hat{x}(\hat{y})$ -magnetizations,  $S^x(S^y) = \frac{1}{2L} \sum_j \langle \psi | \sigma_j^x(\sigma_j^y) | \psi \rangle$  evolve according to:

$$\begin{aligned} S^x((n+1)T) &= \text{Re}[I_n], S^y((n+1)T) = \text{Im}[I_n], \text{ and} \\ I_n &= (-S^y(nT) \cos(\theta_n) + S^z(nT) \sin(\theta_n) + iS^x(nT)) \\ &\quad \exp(-iJ(S^z(nT) \cos(\theta_n) + S^y(nT) \sin(\theta_n))) \end{aligned} \quad (\text{S3})$$

In a manner analogous to the case of the finite size chain, we examine the Fourier spectrum of  $S^z(t)$  to diagnose the dynamical phases of this system (see Fig. S2(a)). We find that in the small  $\epsilon$  regime has a sharp peak at  $\omega = \frac{\pi}{T}$  ( $\omega = \frac{3\pi}{4T}$ ;  $\omega = \frac{\pi}{4T}$ ), thereby signifying the existence of the SOTC-I (SOTC-II) phase; as  $\epsilon$  increases, the system exhibits a transition to the thermal phase.

To complete the analysis of this model, we proceed to determine whether signatures of these phases appear in finite size systems. As shown in Fig. S2, the SOTC-I behavior is clearly visible in small size systems, but the SOTC-II emerges only in large systems.

### EXPERIMENTAL REALIZATIONS

In this section, we discuss three possible experimental realization of our model (Eq. 1 in the main text) in the context of cavity quantum electrodynamics, Bose-Einstein condensates in double-well potentials, and trapped ion crystals.

For the first realization, we study the dynamics of an ensemble of atoms coupled to a single mode cavity. The evolution of the density matrix of the system,  $\hat{\rho}$  in the rotating frame of the atomic transition frequency can be described by the master equation:

$$\frac{d\hat{\rho}}{dt} = -i[\hat{H}_{DH}, \hat{\rho}] + \mathcal{L}_c[\hat{\rho}], \quad (\text{S4})$$

where the Dicke Hamiltonian,  $\hat{H}_{DH}$  is given by

$$\hat{H}_{DH} = \frac{\omega_0}{2} \sum_i \sigma_i^z + \omega \hat{a}^\dagger \hat{a} + g \sum_{i=1}^N (\hat{a}^\dagger + \hat{a}) \hat{\sigma}_i^x \quad (\text{S5})$$

Here  $\omega$  is the atomic transition frequency in the rotating frame,  $\omega_0$  is the cavity mode frequency,  $g$  is the coupling between the atomic spins and the cavity field, and the photon loss from the cavity at a rate  $\kappa$  is given by the Lindblad term:

$$\mathcal{L}_c[\hat{\rho}] = \kappa(2\hat{a}\hat{\rho}\hat{a}^\dagger - \hat{a}^\dagger\hat{a}\hat{\rho} - \hat{\rho}\hat{a}^\dagger\hat{a}). \quad (\text{S6})$$

By adiabatically eliminating the cavity mode in the bad cavity limit ( $\kappa \gg g$ ), we obtain a master equation for the reduced density matrix  $\hat{\rho}_s$  of the spin chain,

$$\frac{d\hat{\rho}_s}{dt} = -i[\hat{H}_{\text{eff}}, \hat{\rho}_s] + \mathcal{L}_\Gamma[\hat{\rho}_s], \quad (\text{S7})$$

where the effective Hamiltonian is given by:

$$\hat{H}_{\text{eff}} = \sum_i \omega \sigma_i^z + \frac{g^2 \omega}{\omega^2 + \kappa^2} \sum_{i,j} \hat{\sigma}_i^x \hat{\sigma}_j^x, \quad (\text{S8})$$

and

$$\mathcal{L}_\Gamma[\hat{\rho}_s] = \frac{g^2 \kappa}{4((\omega - \omega_0)^2 + \kappa^2)} \sum_{i,j} (2\hat{\sigma}_i^- \hat{\rho}_s \hat{\sigma}_j^+ - \hat{\sigma}_i^+ \hat{\sigma}_j^- \hat{\rho}_s - \hat{\rho}_s \hat{\sigma}_i^+ \hat{\sigma}_j^-). \quad (\text{S9})$$

We conclude that the evolution of the spin chain is almost unitary when  $\Delta_c \gg \kappa/2$ . By performing a canonical transformation in this limit, the effective many-body model describing the system is given by Eq. 1, with  $\frac{J}{L} \approx \frac{g^2}{\omega}$  and the quasiperiodic kicks can be implemented by an appropriate magnetic field.

We now examine an alternative route to realize this model. The “all-to-all” interaction can be simulated by a BEC in a double-well potential. The Hamiltonian describing this system is given by:

$$H = g_1 \frac{n_l(n_l + 1) + n_r(n_r + 1)}{2} + g_2 n_l n_r, \quad (\text{S10})$$

where  $n_l(n_r)$  are the number of bosons in the left (right) well. In this case, the kick term can be simulated by tunneling between the two wells:

$$H_{\text{kick}} = \epsilon \tau_n (a_l^\dagger a_r + a_r^\dagger a_l) \delta(t - nT). \quad (\text{S11})$$

Finally, we note that trapped ion quantum emulators provide another platform for realizing our model. In this case, Raman laser beams can generate long-range Ising interactions between the pseudo-spin-1/2 ions. The Hamiltonian describing this system is:

$$H_1 = \sum_{i,j} \frac{J}{|j - i|^\alpha} \sigma_i^x \sigma_j^x \quad (\text{S12})$$

where  $0 \leq \alpha \leq 3$ . Furthermore, arbitrary time-dependent effective magnetic fields are regularly engineered in these experiments [17, 60, 70]. Thus, our predictions can potentially be verified in these systems.

---